

START-TO-END SIMULATIONS OF THz SASE FEL PROOF-OF-PRINCIPLE EXPERIMENT AT PITZ

M. Krasilnikov*, P. Boonpornprasert, F. Stephan, DESY, Zeuthen, Germany
E.A. Schneidmiller, M.V. Yurkov, DESY, Hamburg, Germany
H.-D. Nuhn, SLAC, Menlo Park, California, USA

Abstract

The Photo Injector Test facility at DESY in Zeuthen (PITZ) develops high brightness electron sources for modern linac-based Free Electron Lasers (FELs). The PITZ accelerator has been proposed as a prototype for a tunable, high power THz source for pump and probe experiments at the European XFEL. A Self-Amplified Spontaneous Emission (SASE) FEL is considered to generate the THz pulses. High radiation power can be achieved by utilizing high charge (4 nC) shaped electron bunches from the PITZ photo injector. THz pulse energy of up to several mJ is expected from preliminary simulations for 100 μm radiation wavelength. For the proof-of-principle experiments a re-usage of LCLS-I undulators at the end of the PITZ beamline is under studies. One of the challenges for this setup is transport and matching of the space charge dominated electron beam through the narrow vacuum chamber. Start-to-end simulations for the entire experimental setup - from the photocathode to the SASE THz generation in the undulator section - have been performed by combination of several codes: ASTRA, SCO and GENESIS 1.3. The space charge effect and its impact onto the output THz radiation have been studied. The results of these simulations will be presented and discussed.

INTRODUCTION

The Photo Injector Test facility at DESY in Zeuthen (PITZ) has been suggested as a prototype for developments on an accelerator based high power tunable THz source for pump and probe experiments at the European XFEL [1]. The SASE FEL is considered as main option to generate THz pulses at PITZ using a high bunch charge (4 nC) operation mode of the photo injector. In order to prepare a proof-of-principle experiment start-to-end beam dynamics simulations have been performed. They include generation of electron bunches in the RF photogun, further acceleration by the booster cavity, further transport (~ 25 m) of the space charge dominated electron beam and its matching into the undulator section. A measured field profile of a typical LCLS-I undulator has been used to reconstruct a 3D magnetic field map used for the beam transport through the undulator section. Best obtained matching solution was used to simulate THz SASE FEL with a centre radiation wavelength of ~ 100 μm .

RF GUN AND BOOSTER

The PITZ RF photogun with a peak cathode field of 60 MV/m operated at the launch phase of maximum mean momentum gain (MMMG) is used to generate 4 nC electron bunches by applying photocathode laser pulses with a flattop temporal profile (21.5 ps FWHM) and with a radially homogeneous transverse distribution. Preliminary emittance optimization yielded the optimum photocathode laser spot size which is larger than the whole cathode size. In order to be closer to the practical case a 5 mm diameter of the photocathode laser spot (coinciding with the size of the photocathode) has been used for further optimizations. Beam mean longitudinal momentum of ~ 16.7 MeV/c required for generating THz radiation with ~ 100 μm radiation wavelength is achieved using a booster cavity. For each booster gradient (peak electric field) the booster phase (w.r.t. MMMG) was tuned in order to yield the required final mean momentum of electron beam. Corresponding curve is shown in Fig. 1a. Besides the mean beam momentum booster cavity gradient and phase were tuned in order to yield a small correlated energy spread ($\langle zE \rangle \rightarrow 0$) of the electron beam close to the undulator ($z=29$ m). This two-fold optimization resulted in a peak booster field of 12.85 MV/m and a phase of -26 deg. w.r.t. MMMG (Fig. 1a). The main gun solenoid was tuned to control electron beam size and emittance. Beam dynamics simulations were performed using the ASTRA code [2] with 200000 macroparticles. Simulated rms normalized emittance at the location of the first emittance measurement station (EMSY1 at $z=5.277$ m) is shown in Fig. 1b for the booster MMMG phase and for the optimized correlated energy spread (working point, WP). The chosen absolute value of the gun solenoid peak field of the main solenoid (212.85 mT) is by $\sim 5\%$ lower than that delivering the minimum emittance for the booster in on-crest operation. Corresponding curves of the beam projected transverse emittance and correlated energy spread along the beam line are shown in Fig. 1c. The WP setup corresponds to a more flat emittance along the beamline, whereas a significant increase of the emittance after the minimum is clearly seen for the case of the MMMG booster phase.

Transverse and longitudinal phase spaces of the optimized electron beam (WP) at the EMSY1 location are shown in Fig. 2. This beam setup was used as a starting point for studies on the space charge dominated beam transport towards the undulator section.

* mikhail.krasilnikov@desy.de

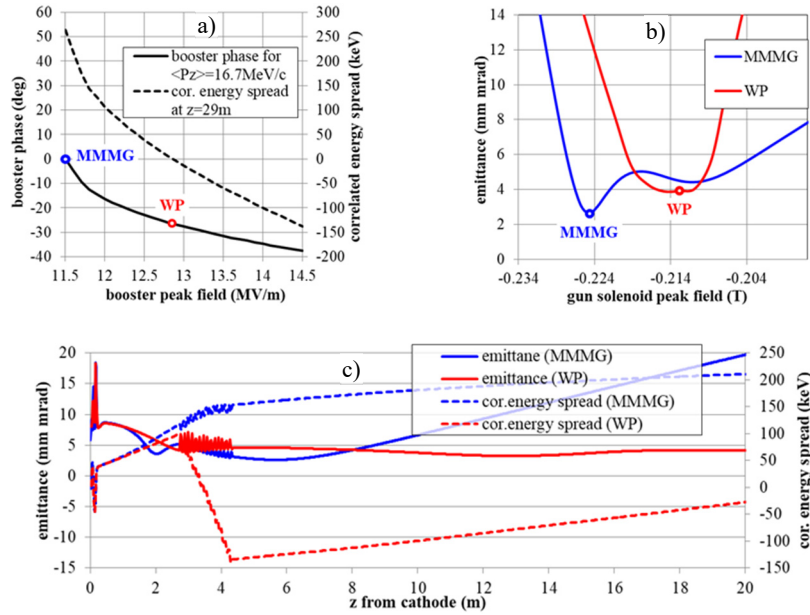


Figure 1: Optimization of RF gun and booster. a) Booster phase w.r.t. MMMG delivering the final beam mean momentum of 16.7 MeV/c. The correlated energy spread at $z=29$ m is shown at the right axis. b) Beam transverse normalized rms emittance at EMSY1 as a function of gun solenoid peak field. c) Beam transverse emittance and correlated energy spread along the beam line simulated for points marked in a) and b).

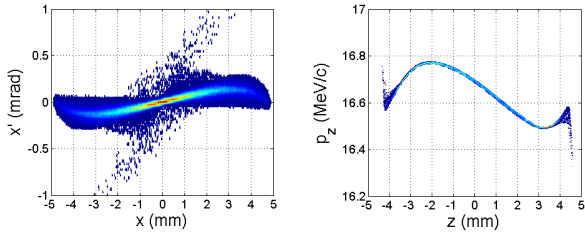


Figure 2: Transverse (left) and longitudinal (right) phase spaces of electron beam at $z=5.277$ m.

BEAM TRANSPORT TO UNDULATOR

Currently for a proof-of-principle SASE THz experiment the installation of LCLS-I undulators is foreseen in the PITZ tunnel annex. The concrete wall between main and annex tunnels is 1.5 m thick and starts at ~ 24 m w.r.t. the photocathode plane. This space is considered for electron beam drift only without any focusing elements inside and assuming a standard beam pipe ($\varnothing 35$ mm). The beam transport through the undulator vacuum chamber (a race-track profile with 5×11 mm cross section and 3.4 m length [3]) is an even much harder task. In order to test a feasibility of such a transport a fast space charge tracking code Space Charge Optimizer (SCO) [4] was used. The results of ASTRA tracking till EMSY1 position (5.277 m) were used as an input for the SCO by applying a corresponding interface. Three triplets of quadrupole magnets were involved into optimization, first two of them were chosen from the magnets available in the present PITZ beamline, and the last one was assumed to be installed at the end of the main tunnel. The solution obtained from the optimized SCO tracking was plugged into the ASTRA

input lattice. Results of SCO and ASTRA simulations are shown in Fig. 3 demonstrating a rather good agreement despite the SCO includes only linear space charge forces.

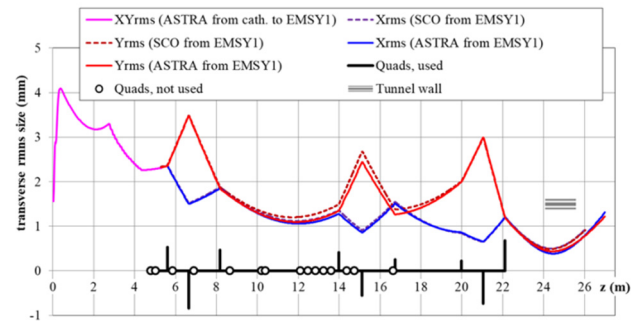


Figure 3: Electron beam rms size along the accelerator simulated using SCO and ASTRA. Gradients of applied quadrupoles are shown schematically on bottom. Circles denote available (but not used) quadrupoles.

MODELING OF UNDULATOR FIELD

The LCLS-I undulator module is a 3.4-m-long permanent magnet planar hybrid structure with 113 periods of $\lambda_U = 30$ mm and a magnetic gap of 6.8 mm [3]. The on-axis field measurements data for SN07 undulator [5] was used to reconstruct a 3D field map required for particle tracking. The undulator peak on-axis field is 1.28 T which corresponds to the undulator parameter of $K=3.585$. Applying Fourier transformation to the measured field profile $B_y(x=0, y=0, z)$ centered around $z=0$ ($|z| \leq L/2$) the vertical component of the magnetic field reads:

$$B_y(0,0,z) = \sum_{n=0}^{\infty} \{a_n \cos(k_n z) + b_n \sin(k_n z)\}, \quad (1)$$

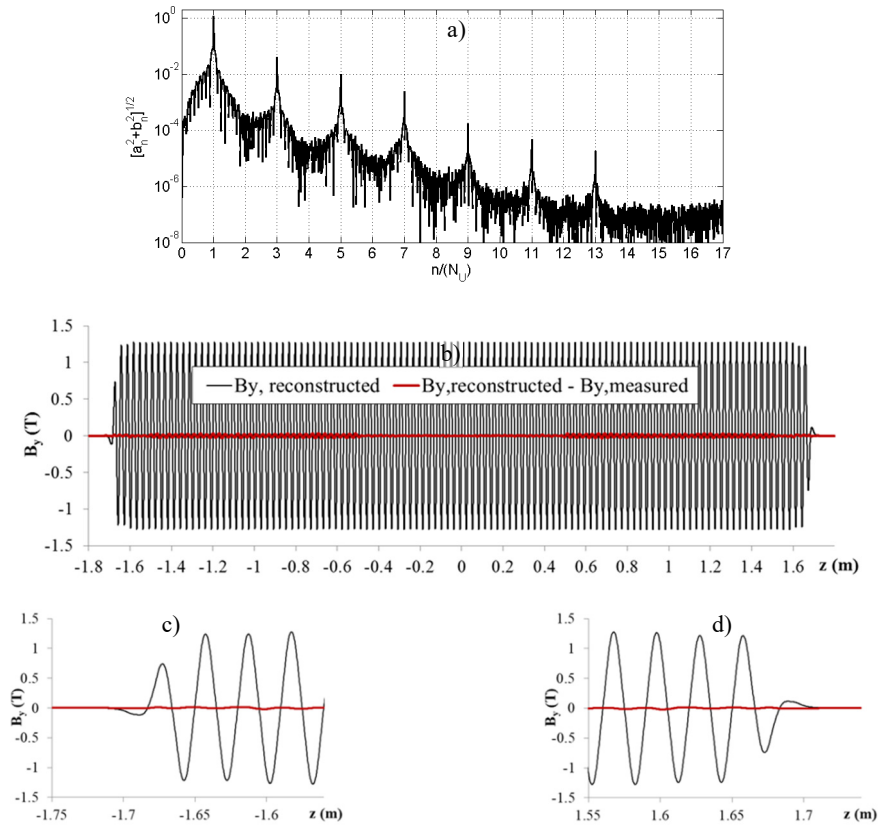


Figure 4: a) Fourier spectrum of the measured undulator field. b) Reconstructed field profile compared with its discrepancy to the measured data. Zoom of the left (c) and right (d) edges of the field profile.

where $L = N_U \lambda_U$ is the undulator effective length and $k_n = 2\pi n/L$ is the wavenumber of the n -th Fourier harmonic. Specific shape of the field profile, including spectral content of the regular periods and the end poles length and strength slope require rather large number of harmonics N_h to be taken into account to reproduce the measured field profile with sufficient accuracy. Proper centring and fine treatment of the measured field profile yield vanishing first and second field integrals. This corresponds to conditions $a_n \approx 0$ and $\sum_{n=1}^{\infty} [(-1)^n b_n/n] \approx 0$ for the first and second integral, correspondingly. These optimization resulted in $L = 120\lambda_U$ (despite nominally the undulator contains only 113 periods) and $N_h = 17$ is a harmonic number of the fundamental wavelength λ_U . This corresponds to the first 2040 ($N_U N_h$) terms of the series (1) taken into account. Fourier spectrum and the field profile reconstructed from it are shown in Fig. 4.

Using a 2D approximation (i.e. no field variation in the horizontal direction) the field satisfying Maxwell's equations can be written as follows:

$$B_y = \sum_{n=1}^{N_h \cdot N_U} \{[a_n \cos(k_n z) + b_n \sin(k_n z)] \cdot \cosh(k_n y)\}, \quad (2)$$

$$B_z = \sum_{n=1}^{N_h \cdot N_U} \{[b_n \sin(k_n z) - a_n \cos(k_n z)] \cdot \sinh(k_n y)\}.$$

Equation (2) has been applied to create 3D field maps of the undulator for their subsequent use in ASTRA and CST Particle Studio [6]. Field imported into the CST is shown in Fig. 5 where the right edge of the structure is depicted. A static magnetic field option of 3D cavity name list was used in ASTRA [2] to simulate particle dynamics in the undulator.

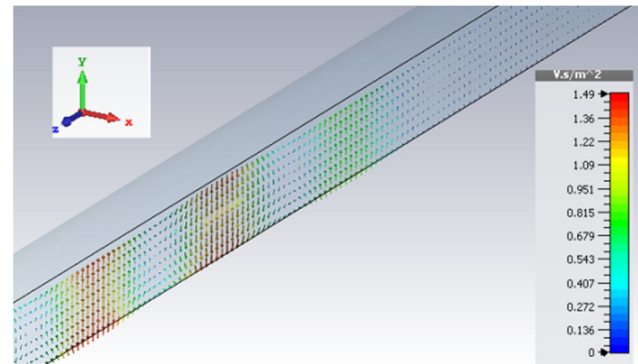


Figure 5: CST model of the undulator field.

The results of the on-axis reference particle tracking by the two above mentioned simulation tools coincide within good accuracy (Fig. 6).

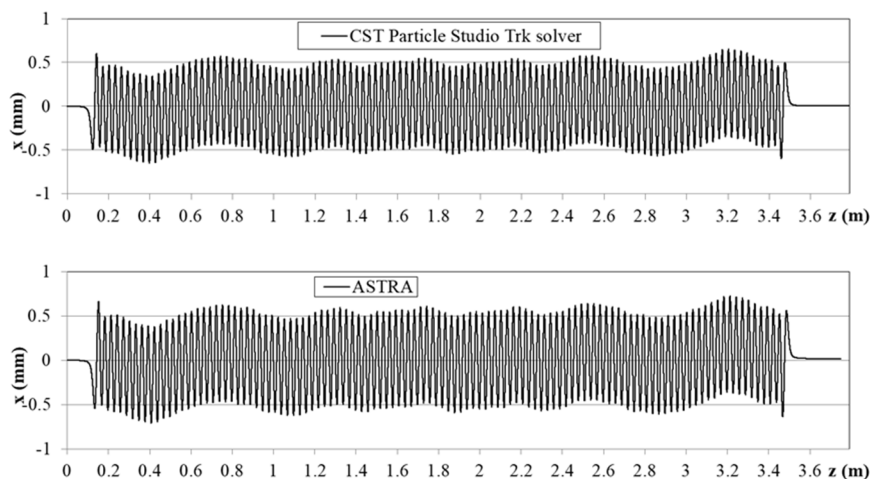


Figure 6: Horizontal trajectory of the on-axis reference particle simulated by: CST Particle Studio Trk solver (upper plot) and ASTRA code (bottom plot).

Off-axis reference particle tracking revealed rather strong vertical focusing by the undulator field (2). The results of these tracking were used for the 4 nC beam matching into the undulator. As a first approximation an ideal model electron distribution with a flat-top temporal (7 mm FWHM) and Gaussian transverse phase spaces (projected emittance of 4 mm mrad) was used. After tuning of the input beam Twiss parameters by running ASTRA an optimum setup has been found (Fig. 7). Results of this matching have shown that for the optimum beam transport through the undulator the electron beam should be rather X-Y asymmetric.

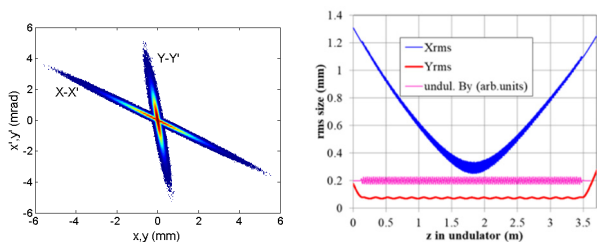


Figure 7: Matching of the model beam into the undulator: left - input transverse phase spaces; right - rms sizes of electron beam in the undulator simulated by ASTRA.

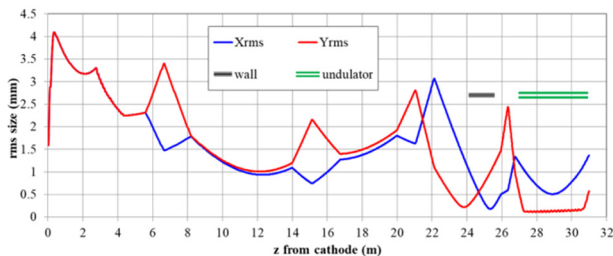


Figure 8: Beam transport in the PITZ linac, including wall and undulator section (ASTRA simulations).

Obtained input parameters were used for the optimization with a beam tracked from the cathode. Finally, undulator section has been included as well. In order to prepare asymmetric matching into the undulator keeping reasonable size of the electron beam inside the wall between the

main tunnel and the annex several quadrupoles were retuned. Results of these optimizations are shown in Fig. 8. Transverse and longitudinal phase spaces of electron beam as well as its slice parameters at the undulator entrance are shown in Fig. 9.

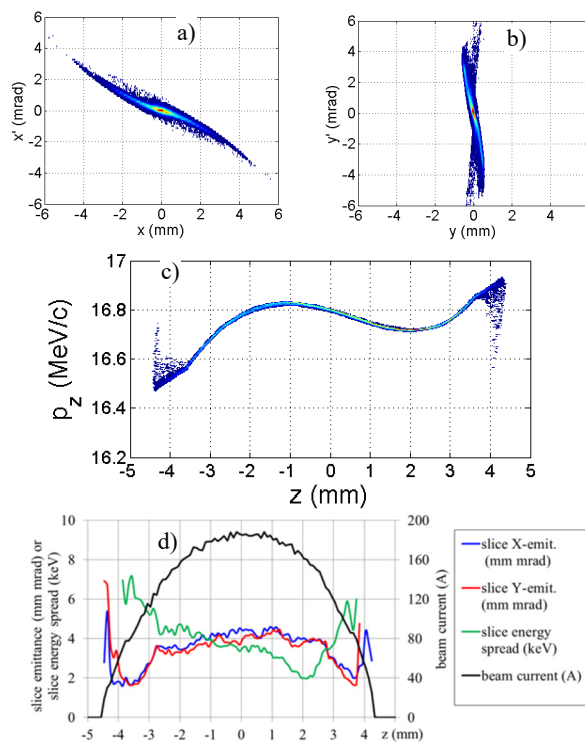


Figure 9: Phase space of the electron beam at the undulator entrance: a) horizontal, b) vertical, c) longitudinal. d) Slice parameters of electron bunch: beam current, slice emittance and slice energy spread.

THz SASE FEL SIMULATIONS

Electron beam parameters (Fig. 9) were used to simulate THz SASE FEL with GENESIS 1.3 code [7]. Only fundamental wavelength λ_U of the undulator field was included. Number of undulator periods was set to 113; no

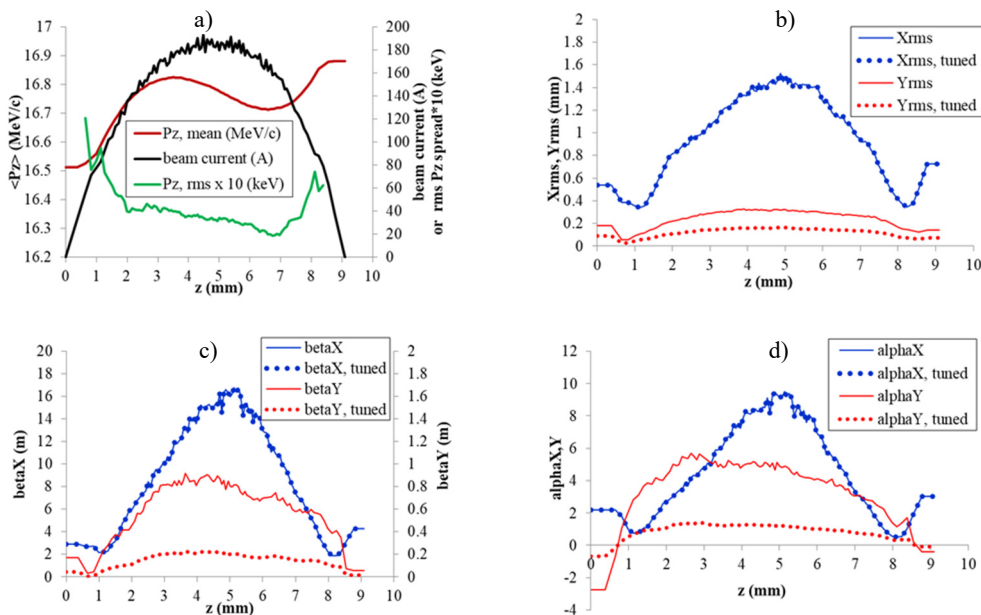


Figure 10: Input electron beam parameters used for GENESIS simulations: a) beam current, mean momentum and slice rms momentum spread; b) transverse rms sizes along the bunch; c) beta functions; d) alpha functions along the bunch.

end cell features were included. Due to these and some other systematic limitations of the simulation tool (e.g., simplified space charge model) an additional tuning w.r.t. input electron beam Twiss parameters was performed to maximize the output THz pulse energy. Mainly vertical Twiss parameters of the input electron beam (β_y, α_y) were varied by simultaneous scaling of corresponding slice parameters. The emittance (slice and projected) remained unchanged. Main beam parameters along the electron bunch are shown in Fig. 10 for the electron beam directly plugged from the start-to-end simulations (nominal beam) and for the beam with (β_y, α_y) scaled by a factor of 0.25 (tuned beam).

Results of GENESIS 1.3 simulations using both input beams are shown in Fig. 11. Grey curves refer to single shot realizations, the black curve corresponds to the average over a hundred realizations (simulation seeds). Only one LCLS-I undulator was used for these simulations. The output THz average pulse energy of 440 μ J for the nominal beam was increased to 600 μ J by the above mentioned tuning of the vertical Twiss parameters of the input electron beam. Average THz pulse at the undulator exit (middle plots in Fig. 11) has peak power of 32 and 38 MW for nominal and tuned beam correspondingly, the

rms duration for both cases is ~ 6 ps. The average spectrum (black curves in the bottom plots of Fig. 11) has a centre at $\sim 107 \mu$ m and a width of $\sim 5 \mu$ m (FWHM). Main parameters of THz pulses obtained from the statistical analysis of hundred realizations are summarized in the Table 1. This includes also an arrival rms time jitter of ~ 1 -2 ps calculated from the centre positions of simulated THz pulses.

Previous simulations of the THz SASE FEL for the PITZ setup with APPLE-II type undulator [8] yielded rather high level of the radiation pulse energy (up to ~ 3 mJ at 100 μ m wavelength). Current start-to-end simulations of the proof-of-principle experiment resulted in a reduction of this level by a factor of 5. This can be related to the planar type of the LCLS-I undulator in contrary to the helical undulator APPLE-II used in [8]. The planar undulator assumes asymmetric beam matching and therefore less efficient interaction of electrons with radiated field, whereas for the helical undulator the focusing in both transverse planes makes this interaction more homogeneous and efficient. Another source of the reduced THz power output is space charge effect, which should be taken into account by matching and transport of 4 nC and 16 MeV electron bunches in the narrow undulator gap.

Content from this work may be used under the terms of the CC BY 3.0 licence (© 2018). Any distribution of this work must maintain attribution to the author(s), title of the work, publisher, and DOI.

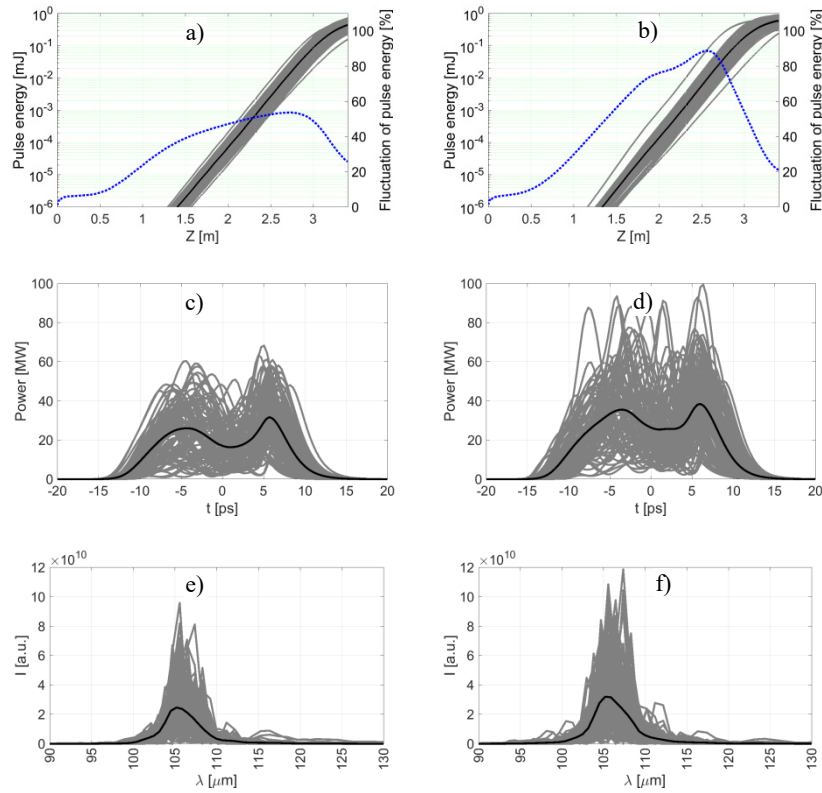


Figure 11: Results of THz SASE FEL simulations with GENESIS code. Pulse energy along the undulator for the nominal (a) and tuned (b) beams. The blue dotted line shows the fluctuation of the pulse energy along the undulator axis. Radiation pulse profile at the undulator exit for the nominal (c) and tuned (d) beams. Corresponding spectra at the undulator exit for the nominal (e) and tuned (f) beams.

Table 1: Simulated THz radiation properties

Parameter	Nominal beam	Tuned beam
Pulse energy (mJ)	0.44±0.11	0.60±0.13
Peak power (MW)	43.0±10.2	58.5±14.3
Pulse rms duration (ps)	5.6±0.7	5.7±0.7
Arrival rms time jitter (ps)	1.7	1.4
Centre wavelength (μm)	106.5	106.8
Spectrum width FWHM (μm)	4.5	4.8

CONCLUSIONS AND OUTLOOK

Start-to-end beam dynamics simulations have been performed for the proof-of-principle experiment on THz SASE FEL generation at PITZ by using a LCLS-I undulator. Space charge dominated electron beam transport through the PITZ accelerator was optimized combining and iterating ASTRA and SCO codes. A model to generate 3D magnetic field map of the undulator has been developed and implemented. Tracking of the reference particle in the undulator field using CST Trk solver and ASTRA yields similar results. A strategy for the matching of

the 4 nC electron bunch into the planar undulator was proposed. Asymmetric beam matching obtained with Gaussian beam was applied to the electron beam tracked from the photocathode and refined by tracking in the undulator field with included space charge effect. Obtained electron beam 6D phase space at the undulator entrance was used as an input for the THz SASE FEL simulations by means of GENESIS 1.3. Additional tuning by scaling of electron beam vertical phase space resulted in the simulated THz pulse energy increase from 440 μJ to 600 μJ at the centre wavelength of ~100 μm. Several effects are still not considered: possible impact of the narrow vacuum chamber of the undulator (wakefield of electron bunch and waveguide effect of the FEL process). Also the space charge model used in ASTRA and GENESIS simulations inside undulator has a limited applicability. Impact of possible undulator imperfections onto beam transport and FEL radiation has still to be estimated as well.

ACKNOWLEDGEMENTS

The authors would like to thank Vladimir Balandin and Nina Golubeva for helpful discussions on simulations of the beam trajectory in undulator.

REFERENCES

- [1] E. Schneidmiller *et al.*, “Tunable IR/THz source for pump probe experiment at European XFEL,” in *Proc. FEL'12*, Nara, Japan, 2012, pp. 503-506.
- [2] ASTRA particle tracking code.
<http://www.desy.de/~mpyf1o/>.
- [3] LCLS Conceptual Design Report, SLAC-R-593, UC-414.
- [4] A. V. Bondarenko, A. N. Matveenko, “Implementation of 2D-emittance compensation scheme in the BERLinPro injector”, in *Proc. FEL'11*, Shanghai, China, 2011, pp. 564–567.
- [5] LCLS Undulator Segment Measurement Results, L143-112000-007.
- [6] Computer Simulation Technology, Darmstadt, Germany: CST Studio. <http://www.cst.com>.
- [7] S. Reiche, "GENESIS 1.3 User Manual" 2004.
<http://genesis.web.psi.ch/index.html>
- [8] P. Boonpornprasert, M. Krasilnikov, and F. Stephan, “Calculations for a THz SASE FEL based on the measured electron beam parameters at PITZ”, in *Proc. FEL'17*, Santa Fe, NM, USA, Aug. 2017, pp. 419-421.